DPNU-03-04
TU-683
UT-ICEPP 03-02
March 2003

Predictions of top and Higgs masses in the top mode standard model with extra dimensions

Michio Hashimoto,[1,*] Masaharu Tanabashi,[2,†] and Koichi Yamawaki[3,‡]
[1]ICEPP, the University of Tokyo, Hongo 7-3-1, Bunkyo-ku, Tokyo 113-0033, Japan
[2]Department of Physics, Tohoku University, Sendai 980-8578, Japan
[3]Department of Physics, Nagoya University, Nagoya 464-8602, Japan
(Dated: March 18, 2003)

We study masses of the top-quark and the Higgs boson in the top mode standard model with extra dimensions, where the standard model gauge bosons and the third generation of quarks and leptons are put in $D(=6,8,10,\cdots)$-dimensions. We analyze the most attractive channel (MAC) by using the renormalization group equations (RGEs) of the gauge couplings. The binding strength of the MAC, of course, should exceed the critical binding strength for the dynamical electroweak symmetry breaking (DEWSB). We can determine the effective cutoff as the energy scale where the DEWSB takes place. We then find that the tau-condensation is favored in the minimal model with $D=6$, while the top-condensate can be the MAC in models with $D=8$ and $D=10$. Combining RGEs for the top-Yukawa and Higgs-quartic couplings with the compositeness conditions, we can predict the top-quark mass m_t and the Higgs boson mass m_H, $m_t = 172-177$ GeV, $m_H = 179-202$ GeV for $D=8$, and $m_t = 166-172$ GeV, $m_H = 181-216$ GeV for $D=10$, where we took the universal compactification scale $1/R = 1-100$ TeV. Our predictions for m_t are successful and our Higgs boson can be observed at collider experiments in near future.

PACS numbers: 11.15.Ex,11.10.Kk,11.25.Mj,12.60.Rc

I. INTRODUCTION

The gauge interaction properties of the Standard Model (SM) have been confirmed quite precisely in the last decade. However, the Higgs particle has not yet been discovered in spite of much effort. The physics behind the electroweak symmetry breaking (EWSB) and the origin of masses of quarks and leptons are left as unresolved problems. The idea of the top quark condensate [1, 2] explains naturally the large top-quark mass of the order of the EWSB scale. This model is often called the "top mode standard model" (TMSM), because the scalar bound state of $\bar{t}t$ plays the role of the Higgs boson in the SM.

In the original version of the TMSM, the 4-top-quark interaction is introduced by hand in order to trigger the EWSB. In addition, the top quark mass m_t is predicted about 10%–30% larger than the experimental value, even if we take the ultraviolet (UV-) cutoff (or the compositeness scale) to the Planck or the GUT scale [1, 3, 4]. Such a huge cutoff also causes a serious fine-tuning problem. For a recent comprehensive review of the top-quark condensation, see, e.g., Ref. [5].

Recently, Arkani-Hamed, Cheng, Dobrescu, and Hall (ACDH) [6] proposed an interesting version of the TMSM in extra dimensions in the spirit of large scale compactification scenario [7]: The SM gauge bosons and the third generation of quarks and leptons live in the $D(=6,8,\cdots)$-dimensional bulk, while the first and second generations are confined in the 3-brane (4 dimensions). Since gauge couplings in higher dimensions than four have negative mass dimension, scattering amplitudes in the bulk at the tree level approximation reach the unitarity bound in a certain high-energy region. Namely, bulk gauge interactions become naively non-perturbative in the high-energy region. Thus, the bulk QCD can trigger the top-condensation without adding 4-fermion interactions in the bulk, in contrast to the original version of the TMSM. However, ACDH did not analyze concretely the dynamics of the bulk QCD. Since we can find easily that the bulk QCD coupling has an upper bound within the same $\overline{\rm MS}$ scheme of the trun-

*E-mail: michioh@post.kek.jp
†E-mail: tanabash@tuhep.phys.tohoku.ac.jp
‡E-mail: yamawaki@eken.phys.nagoya-u.ac.jp

cated Kaluza-Klein (KK) effective theory [8, 9] as that ACDH was based on, it is quite non-trivial whether the top-condensation actually realizes or not. [10] Thus, we have studied the dynamical chiral symmetry breaking (DχSB) and the phase structure in vector-like gauge theories with extra dimensions in the previous papers [10, 11]. We then found that the simplest version of the ACDH scenario with $D = 6$ is unlikely to work, because the bulk QCD coupling cannot become sufficiently large to trigger the top-condensation in the case of $D = 6$ and $n_g = 1$, where n_g denotes the number of generations in the bulk. In addition, we showed that the top-condensation can be realized in the case of $D = 8$ and $n_g = 1$ within the analysis including only the effect of the bulk QCD.

In this paper, we predict the masses of the top quark (m_t) and the Higgs boson (m_H) in the approach á la Bardeen, Hill, and Lindner [3] based on RGEs and the compositeness conditions. Although we have taken into account only the effect of the bulk QCD in the previous works, we make analysis including 1-loop effects of all SM gauge bosons in the bulk. Our scenario works when the top-condensate is the most attractive channel (MAC) [12] and its binding strength κ_t at the cutoff Λ exceeds the critical binding strength $\kappa_D^{\rm crit}$ at the same time,

$$\kappa_t(\Lambda) > \kappa_D^{\rm crit} > \kappa_b(\Lambda), \kappa_\tau(\Lambda), \cdots , \qquad (1)$$

where κ_b and κ_τ denote the binding strengths of the bottom-, and tau-condensates, respectively. We assume that values of $\kappa_D^{\rm crit}$ are not so much changed from previously estimated ones in Ref. [10, 11], even if we incorporate all SM gauge bosons. In our approach, we can determine the cutoff Λ as the energy scale where the top-condensation takes place. Thus, we can also predict the mass of the top-quark as well as the Higgs boson mass, in sharp contrast to the earlier approaches of ACDH [6] and Kobakhidze [13] where the cutoff Λ is treated as an adjustable parameter. We also find that the DχSB takes place in the energy scale close to the Landau pole of the bulk $U(1)_Y$ interaction. When the bulk $U(1)_Y$ interaction becomes quite large, of course, the tau-condensation is favored, instead of the top-condensation. Although ACDH analyzed the MAC under the assumption that all gauge couplings in the bulk are equal, it is obviously insufficient in the above situation. We thus reanalyze more precisely the MAC by using RGEs of gauge couplings. We then find that the tau-condensation is favored in the model with $D = 6, n_g = 1$, while the top-condensate can be the MAC in models with $D = 8, 10, n_g = 1$. We solve RGEs for the top-Yukawa and Higgs-quartic couplings with the compositeness conditions at the effective cutoff where the top-quark in the bulk condenses. We then obtain the top quark mass and the Higgs boson mass,

$$m_t = 172 - 177 \text{ GeV}, \; m_H = 179 - 202 \text{ GeV} \quad (2)$$

for $D = 8, n_g = 1$, and

$$m_t = 166 - 172 \text{ GeV}, \; m_H = 181 - 216 \text{ GeV} \quad (3)$$

for $D = 10, n_g = 1$, where we took the universal compactification radius $R^{-1} = 1 - 100$ TeV and the error range of the strong coupling constant as $\alpha_3(M_Z) = 0.1172 \pm 0.0020$ [14]. We also find that the value of m_t at $1/R$ is governed by the quasi infrared fixed point (IR-FP) for the top-Yukawa coupling y_* [15, 16], which is approximately obtained as $y_* = g_3 \cdot \sqrt{C_F(6+\delta)/(2^{\delta/2} N_c)}$ with the number of color $N_c(= 3)$, the quadratic Casimir of the fundamental representation $C_F(= 4/3)$, and $\delta \equiv D - 4$. The suppression factor $2^{\delta/2}$ in y_* arises from 1-loop corrections of the bulk top-quark to the wave function renormalization constant of the composite Higgs field. The condensation of the bulk top-quark is thus essential so as to obtain $m_t = 170 - 180$ GeV. This is a reason why we can resolve the problem of $m_t \gtrsim 200$ GeV by extending the TMSM into extra dimensions.

The paper is organized as follows. In Sec.2, we study running effects of gauge couplings in the bulk. In Sec.3, we identify the MAC and find the effective cutoff at which the DχSB takes place. In Sec.4, we predict m_t and m_H. Sec.5 is devoted to summary and discussions. In Appendix A, we present a concrete procedure of our compactification. We also show the numerical calculation for the total number of KK modes below the renormalization point.

II. RUNNING EFFECTS OF BULK GAUGE COUPLINGS

We consider that the SM gauge group and the third generation of quarks and leptons are put in D dimensional bulk, while other first and second generations live on the 3-brane (4-dimensions). (ACDH model [6]) Here, we assume that four of D-dimensions are the usual Minkowski spacetime and extra $(D - 4)$ spatial dimensions are compactified at a universal scale $1/R$ of the order of a few TeV. Since we investigate chiral condensations of bulk fermions, we take even dimensions, $D = 6, 8, 10, \cdots$.

Before analyzing the most attractive channel (MAC) [12] at the cutoff scale Λ, we study running effects of bulk gauge couplings. For a while, we consider an effective theory on the 3-brane. Below the compactification scale $1/R$, renormalization group equations (RGEs) of gauge couplings $g_i (i = 3, 2, Y)$ on the 3-brane are, of course, reduced into the SM one,

$$(4\pi)^2 \mu \frac{dg_i}{d\mu} = b_i \, g_i^3, \quad (\mu < 1/R) \tag{4}$$

with $b_3 = -7, b_2 = -\frac{19}{6}$ and $b_Y = \frac{41}{6}$. However, we should take into account contributions of Kaluza-Klein (KK) modes in $\mu \geq 1/R$. Since the KK modes heavier than the renormalization scale μ are decoupled in RGEs on the 3-brane, we only need summing up the loops of the KK modes lighter than μ. This is called "truncated KK" effective theory [8, 9]. Within the truncated KK effective theory, we obtain RGEs for gauge couplings $g_i (i = 3, 2, Y)$ on the 3-brane:

$$(4\pi)^2 \mu \frac{dg_i}{d\mu} = b_i \, g_i^3 + N_{\rm KK}(\mu) \, b_i' \, g_i^3, \quad (\mu \geq 1/R) \tag{5}$$

where $N_{\rm KK}(\mu)$ denotes the total number of KK modes below the renormalization point μ. We easily find

$$N_{\rm KK}(\mu) = \frac{1}{2^n} \frac{\pi^{\delta/2}}{\Gamma(1+\delta/2)} (\mu R)^\delta, \quad \delta \equiv D - 4 \tag{6}$$

for $\mu \gg R^{-1}$ with the orbifold compactification T^δ / Z_2^n. Hereafter, we take Z_2 projection for $D = 6$, $Z_2 \times Z_2'$ projection for $D = 8$, and $Z_2 \times Z_2' \times Z_2''$ projection for $D = 10$ [1], i.e.,

$$n = 1, 2, 3 \tag{7}$$

for $D = 6, 8, 10$, respectively. In Appendix A, we show the numerical calculation of $N_{\rm KK}(\mu)$. The RGE coefficients b_i' arising from loop effects of KK modes are obtained as

$$b_3' = -11 + \frac{\delta}{2} + \frac{4}{3} \cdot 2^{\delta/2} \cdot n_g \tag{8}$$

for $SU(3)_c$,

$$b_2' = -\frac{22}{3} + \frac{\delta}{3} + \frac{4}{3} \cdot 2^{\delta/2} \cdot n_g + \frac{1}{6} n_H \tag{9}$$

for $SU(2)_W$, and

$$b_Y' = \frac{20}{9} \cdot 2^{\delta/2} \cdot n_g + \frac{1}{6} n_H \tag{10}$$

for $U(1)_Y$, respectively, where n_g (n_H) denotes number of generations (composite Higgs bosons) in the bulk. In our model, n_g is unity and one composite Higgs doublet, $n_H = 1$, is assumed. (In RGE coefficients b_i for the SM, we have already assumed the minimal Higgs sector.) Matching the 3-brane action to the bulk action, we find the relation between the *dimensionfull* bulk gauge coupling g_D and the 3-brane gauge coupling g, $g_D^2 = (2\pi R)^\delta g^2 / 2^n$. On the other hand, it is natural to define the *dimensionless* bulk gauge coupling $\hat{g}$ as $\hat{g}^2 \equiv g_D^2 \mu^\delta$. Thus, we can write down $\hat{g}_i$ in the terms of g_i,

$$\hat{g}_i^2(\mu) = \frac{(2\pi R\mu)^\delta}{2^n} g_i^2(\mu). \tag{11}$$

Substituting Eq. (11) for Eq. (5), we can obtain RGEs for $\hat{g}_i$,

$$\mu \frac{d}{d\mu} \hat{g}_i = \frac{\delta}{2} \hat{g}_i + \frac{\hat{g}_i^3}{(4\pi)^2} \frac{2^n}{(2\pi R\mu)^\delta} \left[b_i + N_{\rm KK}(\mu) b_i' \right]. \tag{12}$$

We solve numerically Eq. (12) and show typical behavior of the dimensionless bulk gauge couplings in Fig. 1. We used input parameters at $\mu = M_Z (= 91.1876 \text{ GeV})$ as [14]

$$\alpha_3(M_Z) = 0.1172, \tag{13}$$

and

$$\alpha_{\rm QED}^{-1}(M_Z) = 127.934, \quad \sin^2\theta_W(M_Z) = 0.23113, \tag{14}$$

whose values correspond to

$$\alpha_2(M_Z) = 0.033813, \quad \alpha_Y(M_Z) = 0.010166. \tag{15}$$

Now, we consider analytical expressions for $\hat{g}_i$. Eq. (12) is approximately written as

$$\mu \frac{d}{d\mu} \hat{g}_i = \frac{\delta}{2} \hat{g}_i + (1 + \delta/2) \Omega_{\rm NDA} b_i' \, \hat{g}_i^3 \tag{16}$$

in $\mu \gg 1/R$, where we used Eq. (6) and defined the loop factor $\Omega_{\rm NDA}$ in D-dimensions,

$$\Omega_{\rm NDA} \equiv \frac{1}{(4\pi)^{D/2} \Gamma(D/2)}. \tag{17}$$

Thus, we easily find that dimensionless bulk gauge couplings with $b_i' < 0$ have ultraviolet fixed points (UV-FPs) g_{i*},

$$g_{i*}^2 \Omega_{\rm NDA} = \frac{1}{-(1 + 2/\delta) \, b_i'}, \tag{18}$$

[1] For a concrete procedure, see Appendix A.

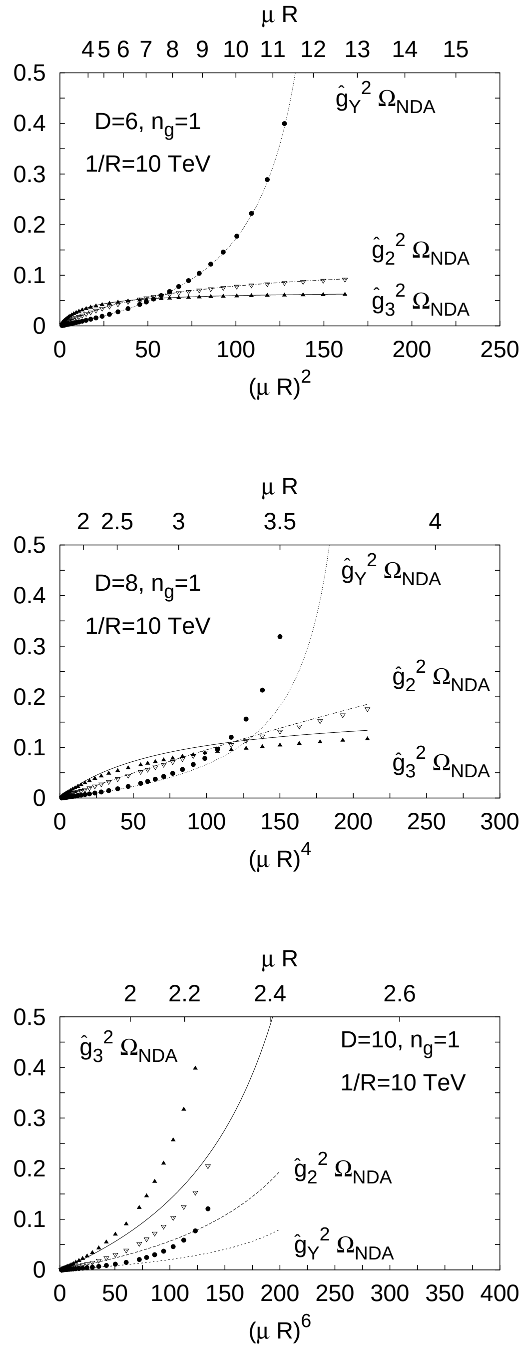

FIG. 1: Typical RG flows of the dimensionless bulk gauge couplings, $\hat{g}_3^2\Omega_{\rm NDA}, \hat{g}_2^2\Omega_{\rm NDA}$, and $\hat{g}_Y^2\Omega_{\rm NDA}$. The graphs from top to bottom show RG flows for $D = 6, 8, 10, n_g = 1, R^{-1} = 10$ TeV, respectively. In all graphs, points and lines represent numerical solutions of Eq. (12) and analytical ones such as Eq. (19). In addition, the upward and downward horizontal lines are the renormalization point μ and $(\mu R)^\delta$ which is closely related to the total number of KK modes below μ, respectively. We used $\alpha_3(M_Z) = 0.1172$, $\alpha_2(M_Z) = 0.033813$, and $\alpha_Y(M_Z) = 0.010166$.

within the truncated KK effective theory. We can also show $b'_3 < 0$ and $\hat{g}_3^2(\mu) \leq g_{3*}^2$ for the bulk QCD with $D = 6, n_g = 1, 2, 3$ and with $D = 8, n_g = 1$. In our previous analyses in Ref. [10, 11], we have studied the dynamics of bulk gauge theories with $b'_i < 0$. In this paper, we include the effect of the bulk hypercharge. Of course, b'_Y is always positive. Even in the bulk QCD, we find that the coefficient b'_3 becomes positive for $D = 8, n_g \geq 2$ and $D \geq 10, n_g \geq 1$. An important point is that gauge theories with $b'_i > 0$ have the Landau pole Λ_{Li}. Within the approximation of Eq. (16), we can rewrite analytically the dimensionless bulk gauge couplings with $b'_i > 0$ as

$$\hat{g}_i^2(\mu)\Omega_{\rm NDA} = \frac{1}{(1+2/\delta)\, b'_i} \cdot \frac{\mu^\delta}{-\mu^\delta + \Lambda_{Li}^\delta}, \quad (19)$$

where the Landau pole Λ_{Li} is given by

$$(\Lambda_{Li} R)^\delta \;=\; 1 + \frac{2^n \delta^2 \Gamma(\delta/2)}{b'_i\, \pi^{\delta/2-1}} \times \left(\alpha_i^{-1}(M_Z) + \frac{b_i}{2\pi}\ln(M_Z R)\right). \quad (20)$$

The similar expression for $\hat{g}_i(\mu)$ with $b'_i < 0$ is shown in Ref. [11]. Since the $SU(2)_W$ interaction does not contribute chiral condensations such as $\langle \bar{t}_L t_R \rangle$, the sign of b'_2 is less important. Here, we comment on validity of analytical expressions such as Eq. (19). Comparing Eq. (19) with numerical solutions of Eq. (12), we find that our approximations work very well for $D = 6, n_g = 1$, whereas they are not numerically so well for $D = 8, 10, n_g = 1$. (See also Fig. 1.) The Landau poles Λ_{Li} are very close to the compactification scale, $\Lambda_{Li} R \sim 2 - 4$ for $D = 8, 10, n_g = 1$. This is the reason why our approximations are broken down. (See also graphs for $N_{\rm KK}(\mu)$ in Appendix A.) Although analytical expressions for $\hat{g}_i^2(\mu)$ such as Eq. (19) describe roughly behaviors of $\hat{g}_i^2(\mu)$, they are not suitable for the numerical analysis. Hereafter, we do not use analytical expressions such as Eq. (19) in numerical calculations.

The bulk hypercharge always has the Landau pole Λ_{LY}. We cannot take the cutoff larger than the Landau pole Λ_{LY}. In addition, the bulk QCD coupling with $D = 10, n_g = 1$ also goes to infinity at its Landau pole Λ_{L3}. Thus, we study the behavior of the bulk QCD coupling $\hat{g}_3$ below the Landau pole Λ_{LY} of the bulk hypercharge. In Fig. 1, we find that the Landau pole Λ_{LY} is not so far from the universal compactification scale $1/R$, e.g. $\Lambda_{LY} R \simeq 13, 3.7, 2.3$ for $D = 6, 8, 10, n_g = 1$, respectively. As shown in Fig. 1, each behavior of $\hat{g}_3$ below Λ_{LY} is quite different in $D = 6, 8, 10$. The bulk QCD coupling around Λ_{LY} is close to its UV-FP g_{3*} in $D = 6, n_g = 1$, whereas $\hat{g}_3$ in $D = 8, n_g = 1$ is well below g_{3*} in the whole energy region $\mu < \Lambda_{LY}$. In the case of $D = 10, n_g = 1$, the Landau pole Λ_{L3} for the bulk QCD coupling is close to that of the bulk hypercharge Λ_{LY}. (See also Fig. 1.)

In any case, we cannot neglect the effect of the bulk hypercharge in the analysis of the MAC. Taking into account the running effects of $\hat{g}_{3,Y}(\mu)$, we study the MAC in the next section.

III. MAC AND CRITICAL BINDING STRENGTH

In this section, we reanalyze the MAC by using the running bulk gauge couplings $\hat{g}_i(\mu)$. If the top quark condensate becomes the MAC and its binding strength exceeds the critical value for the DχSB at the same time, the TMSM in the bulk can be naturally realized within pure bulk gauge theories. In the MAC analysis of the earlier attempt [6], they assumed $\hat{g}_3^2 = \hat{g}_2^2 = \hat{g}_1^2 (= 5/3 \hat{g}_Y^2)$, although these values for $D = 6, 8, n_g = 1$ shown in Fig. 1 look like very small, $\hat{g}_i^2 \sim 0.1$. (The gauge couplings are not unified in strict sense.) In addition, they did not study the dynamics of the bulk gauge interactions. Thus, we have investigated the DχSB in the bulk and estimated the value of the critical binding strength for the DχSB [10, 11]. In the following analysis, we find that the binding strength of the top-condensate reaches the critical value near the Landau pole Λ_{LY} rather than the point of $\hat{g}_3^2 \simeq \hat{g}_2^2 \simeq \hat{g}_1^2$. In such a situation, it is nontrivial whether the top-condensate becomes the MAC or not. Thus, the running effects of $\hat{g}_i(\mu)$ are crucial in our analysis of the MAC. We also note that the cutoff Λ should not be an adjustable parameter like in the approaches of ACDH [6] and Kobakhidze [13], but *it is determined as the energy scale that the DχSB takes place.* Since the cutoff Λ is related to the electroweak symmetry breaking (EWSB) scale through the vacuum expectation value (VEV) of the top-condensate, the scale of Λ is calculable, for example, by using the Pagels-Stokar formula [19], once the EWSB scale v is fixed to $v = 246$ GeV. In this paper, however, we expect that the value of the effective cutoff Λ is around the critical energy scale realizing $\langle \bar{t}t \rangle \neq 0$, instead of calculating Λ explicitly.

At the beginning, we identify the MAC at the cutoff Λ. In the one-gauge-boson-exchange approximation, the binding strength κ of a $\bar{\psi}\chi$ channel is given by

$$\begin{aligned}\kappa(\mu) \equiv\ & \hat{g}_3^2(\mu)\Omega_{\rm NDA} \boldsymbol{T}_{\bar{\psi}} \cdot \boldsymbol{T}_\chi \\ & + \hat{g}_2^2(\mu)\Omega_{\rm NDA} \boldsymbol{T'}_{\bar{\psi}} \cdot \boldsymbol{T'}_\chi \\ & + \hat{g}_Y^2(\mu)\Omega_{\rm NDA} Y_\psi Y_\chi, \end{aligned} \tag{21}$$

where $\boldsymbol{T}$, $\boldsymbol{T'}$ are the generators of $SU(3)_c, SU(2)_W$, and Y is the hypercharge. Noting the identity,

$$\boldsymbol{T}_{\bar{\psi}} \cdot \boldsymbol{T}_\chi = \frac{1}{2}\left(C_2(\bar{\psi}) + C_2(\chi) - C_2(\bar{\psi}\chi) \right) \tag{22}$$

with the quadratic Casimir $C_2(r)$ for the representation r of the gauge group, we can easily calculate the binding strength and obtain

$$\kappa_t(\mu) = C_F \hat{g}_3^2(\mu)\Omega_{\rm NDA} + \frac{1}{9}\hat{g}_Y^2(\mu)\Omega_{\rm NDA} \tag{23}$$

for the top-condensate with the quadratic Casimir $C_F (= 4/3)$ of the fundamental representation,

$$\kappa_b(\mu) = C_F \hat{g}_3^2(\mu)\Omega_{\rm NDA} - \frac{1}{18}\hat{g}_Y^2(\mu)\Omega_{\rm NDA} \tag{24}$$

for the bottom-condensate, and

$$\kappa_\tau(\mu) = \frac{1}{2}\hat{g}_Y^2(\mu)\Omega_{\rm NDA} \tag{25}$$

for the tau-condensate, respectively. Our scenario of the TMSM with extra dimensions works in the situation,

$$\kappa_t(\Lambda) > \kappa_D^{\rm crit} > \kappa_b(\Lambda), \kappa_\tau(\Lambda), \tag{26}$$

where $\kappa_D^{\rm crit}$ denotes the critical binding strength. From Eqs. (23), (24), (25), and binding strengths listed in Ref. [6], we easily find that the MAC is the top (tau)-condensate among many possible scalar bound states, when the bulk QCD (hypercharge) is dominant. Here, we note that we should take a moderately large cutoff Λ, since bulk gauge interactions at the scale of $N_{\rm KK}(\Lambda) \sim \mathcal{O}(1)$ are perturbative. Since the bulk QCD coupling in $D = 6, 8, n_g = 1$ is less than its UV-FP as we have shown in the previous section, the bulk hypercharge becomes dominant near the Landau pole Λ_{LY}. In the cases of $D = 6, 8, n_g = 1$, thus, it is highly non-trivial whether suitable cutoffs realizing only the top-condensation exist or not between $1/R$ and Λ_{LY}.

Next, we discuss the value of the critical binding strength $\kappa_D^{\rm crit}$. In the estimation of $\kappa_D^{\rm crit}$, the naive dimensional analysis (NDA) [17, 18] is usually applied. In the NDA, the DχSB is expected to occur when the binding strength κ is larger than one, i.e.,

$$\kappa_D^{\rm crit}({\rm NDA}) = 1. \tag{27}$$

Our scenario with $D = 10, n_g = 1$ works even in the framework of the NDA up to $1/R \simeq 34$ TeV. For more concrete estimation of $\kappa_D^{\rm crit}$, we have studied the (improved) ladder Schwinger-Dyson (SD) equation in the bulk, which is a gap equation derived from the bi-local 4-fermion interaction. [10, 11] We have incorporated the bulk QCD interaction with $\hat{g}_3^2(\mu) = $ const., whose approximation is justified in $b_3' < 0$ and $\Lambda R \gg 1$ thanks to the UV-FP. In the ladder SD equation, running effects in the whole energy region below the cutoff contribute to the DχSB. As shown in Fig. 1, all of bulk gauge couplings $\hat{g}_i^2(\mu)$ are monotonously increasing functions. Thus, the simplification of $\hat{g}_i^2(\mu) = $ const. leads to lower bounds of critical points for the DχSB. In the analysis of Ref. [10], we have used the so-called Higashijima-Miransky (or improved ladder) approximation [20, 21] in order to incorporate the running effect of the bulk gauge coupling [2]. In the Higashijima-Miransky approximation, we replace the dimensionfull bulk gauge coupling g_D to the running one as

$$g_D^2 \to g_D^2(\max(-p^2, -q^2)), \tag{28}$$

where p and q denote the external and loop momenta of the bulk fermion, respectively. While the improved ladder approximation with the Landau gauge is consistent with the vector Ward-Takahashi (WT) identity, the axial WT identity is violated. However, this approximation has been widely used because it greatly simplifies the angular integration in the ladder SD equation. In the limit of $\Lambda R \gg 1$, we find numerically the critical points with $\kappa(\mu) = $ const.,

$$\kappa_6^{\rm crit}({\rm SD1}) \simeq 0.122 \tag{29}$$

for $D = 6$,

$$\kappa_8^{\rm crit}({\rm SD1}) \simeq 0.146 \tag{30}$$

for $D = 8$, and

$$\kappa_{10}^{\rm crit}({\rm SD1}) \simeq 0.163 \tag{31}$$

for $D = 10$, respectively [3]. In Ref. [11], on the other hand, we have taken the argument of the running coupling to the loop momentum of gluon such as

$$g_D^2 \to g_D^2(-(p-q)^2). \tag{32}$$

This is a manner consistent with the vector and axial WT identities, although it is generally difficult to perform analytically the angular integration in the ladder SD equation. [22] In Ref. [11], we have estimated the critical points $\kappa_D^{\rm crit}$ with $\Lambda R \gg 1$ and $\kappa(\mu) = $ const.,

$$\kappa_D^{\rm crit}({\rm SD2}) = \frac{\rm D}{32}\frac{\rm D-2}{\rm D-1}, \tag{33}$$

whose numerical values are

$$\kappa_6^{\rm crit}({\rm SD2}) = \frac{3}{20} = 0.15 \tag{34}$$

for $D = 6$,

$$\kappa_8^{\rm crit}({\rm SD2}) = \frac{3}{14} \simeq 0.214 \tag{35}$$

for $D = 8$, and

$$\kappa_{10}^{\rm crit}({\rm SD2}) = \frac{5}{18} \simeq 0.278 \tag{36}$$

for $D = 10$, respectively. Although we find numerically $\kappa_D^{\rm crit}({\rm SD2}) \gtrsim \kappa_{\rm D}^{\rm crit}({\rm SD1})$, the D$\chi$SB can take place in both cases, even if the binding strength is about 0.1 times less than the value of the NDA. Here, we note that we cannot take a sufficiently large cutoff due to the Landau pole in fact. In our situation $\Lambda R \sim 1-10$, explicit breaking effects of the D-dimensional Lorentz symmetry due to the compactification may not be negligible. When we take into account such a effect in the estimation of $\kappa_D^{\rm crit}$, we find that the critical point $\kappa_D^{\rm crit}$ tends to be larger [11]. Namely, the value of $\kappa_D^{\rm crit}$ is unlikely to be smaller than $\kappa_D^{\rm crit}({\rm SD1})$, even if we take into account ambiguities of the ladder SD equation about $\sim 20\%$. Thus, we can regard $\kappa_D^{\rm crit}({\rm SD1})$ as the minimal estimation among available values of the critical points. We use most conservatively $\kappa_D^{\rm crit}({\rm SD1})$ in the following analysis.

Now, we are ready to study which of condensations is the MAC and whether the MAC condensation can realize or not. We compare the binding strengths of top-, bottom-, and tau-condensates with the critical point $\kappa_D^{\rm crit}$. (See Fig. 2.) In the model with $D = 6, n_g = 1$, the top-condensation can take place around $(\Lambda R)^2 \gtrsim 125$, while the tau-condensation is realized around $(\Lambda R)^2 \gtrsim 100$. Thus, the minimal scenario of the bulk TMSM with $D = 6, n_g = 1$

[2] The ladder SD equation is written in terms of the dimensionfull bulk gauge coupling g_D.

[3] The value for $D = 10$ is not reported in Ref. [10].

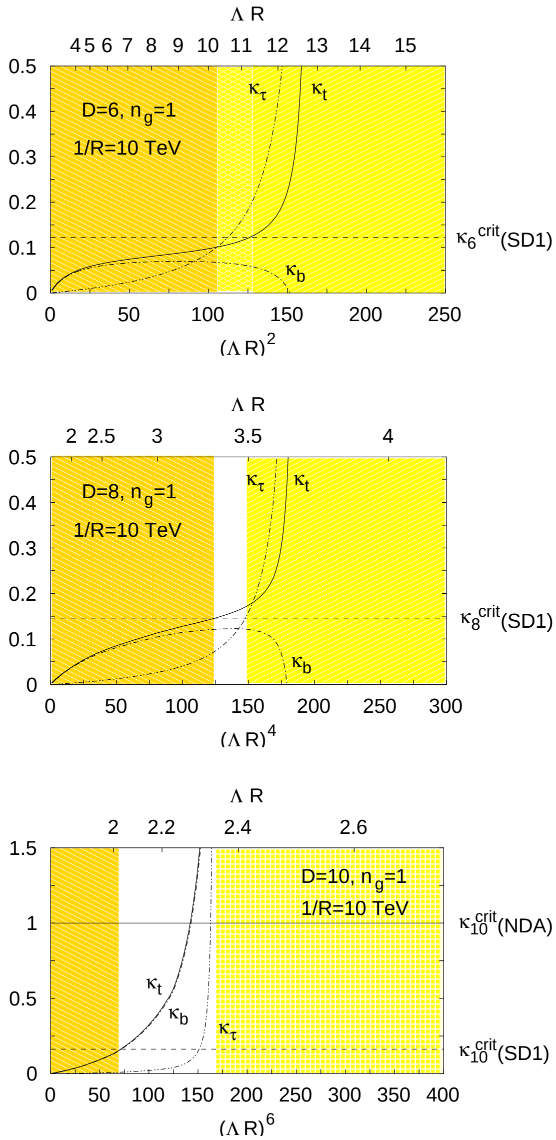

FIG. 2: Effective cutoffs Λ for the top-condensation in the bulk. The graphs from top to bottom represent the binding strength $\kappa_{t,b,\tau}$ with $D = 6, 8, 10, n_g = 1, R^{-1} = 10$ TeV, respectively. The unshaded regions show suitable cutoffs satisfying the condition, $\kappa_t(\Lambda) > \kappa_D^{\rm crit}(\text{SD1}) > \kappa_\tau(\Lambda)$. The shaded region in the R.H.S. of the bottom graph is excluded because of $\Lambda > \Lambda_{LY}$.

is unlikely to work. For $D = 8, n_g = 1$, we find that the condition $\kappa_t(\Lambda) > \kappa_D^{\rm crit}(\text{SD1}) > \kappa_\tau(\Lambda)$ is satisfied by using the effective cutoff, $(\Lambda R)^4 \simeq 125-150$. It is also important that the bottom condensation is naturally suppressed in $D = 8, n_g = 1$. Although the top-condensate becomes the MAC in $D = 10, n_g = 1$ and its binding strength exceeds the critical point $\kappa_{10}^{\rm crit}(\text{SD1})$, we need to tune finely the effective cutoff in order to suppress the bottom condensation. (See also Fig. 2.) We note that these behaviors of the binding strengths, $\kappa_{t,b,\tau}$, are not so changed by varying the compactification scale, $R^{-1} = 1-100$ TeV. (See Figs. 3, 4, and 5.)

In the next section, we predict the top-quark mass m_t and the Higgs boson mass m_H by using the effective cutoff Λ around $\kappa_t(\Lambda) \simeq \kappa_D^{\rm crit}(\text{SD1})$.

IV. PREDICTIONS OF m_t AND m_H

The parameter in our approach is essentially only one, ΛR. In the previous section, we have determined Λ as the energy scale satisfying the relation $\kappa_t(\Lambda) \sim \kappa_D^{\rm crit}(\text{SD1})$. By using such a cutoff Λ and RGEs of the top-Yukawa and Higgs-quartic couplings, we can predict masses of the top-quark and the Higgs boson, m_t and m_H.

As shown in our earlier papers [10, 11], the condensation of the bulk fermion in bulk gauge theories has the large anomalous dimension, $\gamma_m = D/2 - 1$ near the critical point. We thus find that the 4-fermion operator in the bulk becomes a marginal one. The situation is quite similar to the strongly interacting QED in 4-dimensions [23, 24]. Although our model is based on pure bulk gauge theories, 4-fermion operators such as $(\bar{q}_L t_R)^2$ are generated in the bulk. If we assume that the coefficient of the 4-top operator is sufficiently large and attractive, while the 4-bottom and 4-tau interactions are repulsive, the ACDH scenario always works, even in $\kappa_t(\Lambda) < \kappa_D^{\rm crit}$. In such a case, we need to study the phase structure of the gauged Nambu-Jona-Lasinio model in the bulk. The analysis will be performed elsewhere [25]. In this paper, we pursue the possibility that the DχSB takes place thanks to bulk gauge interactions.

We rewrite the 4-top interaction in terms of the composite scalar field by using the auxiliary field method as usual,

$$(\bar{q}_L t_R)^2 \to H_0^\dagger H_0, \tag{37}$$

where H_0 denotes the bare Higgs field. We thereby obtain the bulk SM without the kinetic term for H_0 at the cutoff scale Λ,

$$\begin{aligned} \mathcal{L}_D &= \mathcal{L}_{\rm kin} - y_0(\bar{q}_L H_0 t_R + \text{h.c.}) \\ &\quad - m_{H0}^2 H_0^\dagger H_0 - \frac{\lambda_0}{2}(H_0^\dagger H_0)^2, \end{aligned} \tag{38}$$

where $\mathcal{L}_{\rm kin}$ represents the kinetic terms of the top-quark and gauge bosons in the bulk, and y_0, λ_0 and m_{H0} denote bare quantities. Below

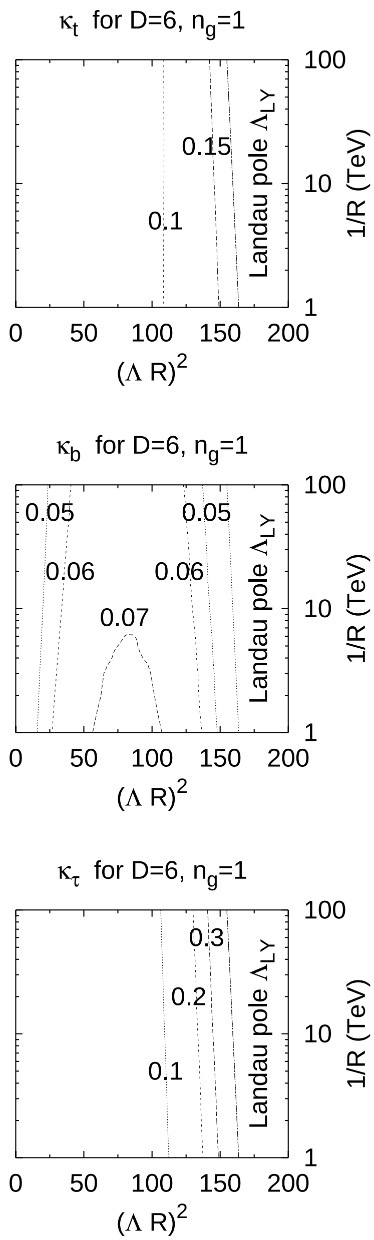

FIG. 3: Dependence of the binding strengths, κ_t, κ_b, and κ_τ, on the compactification scale R^{-1}. In all graphs, the vertical and the horizontal lines are the compactification scale R^{-1} and $(\Lambda R)^\delta$, respectively. We used $\alpha_3(M_Z) = 0.1172$, and $\alpha_Y(M_Z) = 0.010166$.

the cutoff Λ, the composite Higgs field in the bulk develops its kinetic term. In the same way as the approach of the TMSM á la Bardeen, Hill and Lindner [3], we can expect to reproduce the conventional SM in the bulk in the energy scale

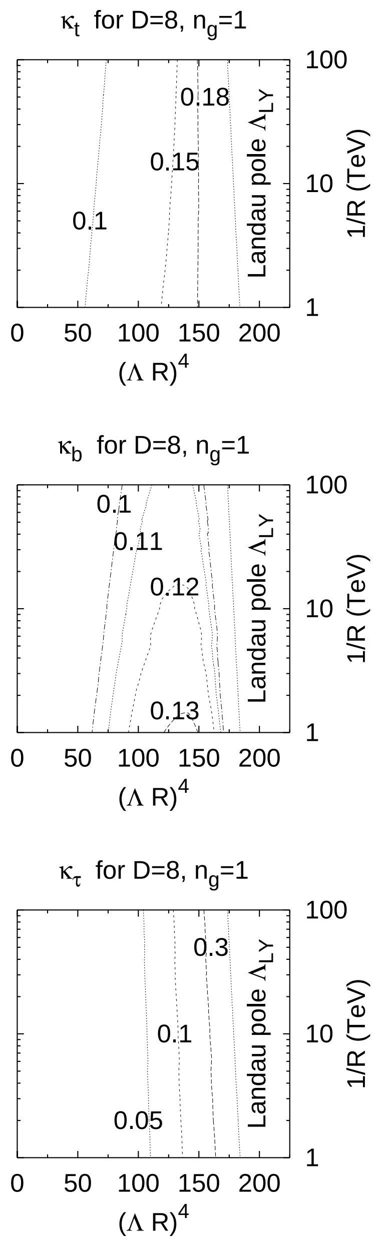

FIG. 4: The same graphs as Fig. 3 in the case of $D = 8, n_g = 1$.

between $1/R$ and Λ:

$$\begin{aligned} \mathcal{L}_D &\to \mathcal{L}_{\rm kin} - y(\bar{q}_L H t_R + \text{h.c.}) \\ &+|D_M H|^2 - m_H^2 H^\dagger H - \frac{\lambda}{2}(H^\dagger H)^2, \end{aligned} \tag{39}$$

where $M = 0, 1, 2, 3, 5, \cdots D$, and we renormalized bare couplings as

$$y = Z_y y_0/(Z_H^{1/2} Z_{q_L}^{1/2} Z_{t_R}^{1/2}), \lambda = Z_\lambda \lambda_0 / Z_H^2 \tag{40}$$

by using the multiplicative renormalization of the fields, $H_0 \to H/Z_H^{1/2}, q_L \to q_L/Z_{q_L}^{1/2}$, and $t_R \to t_R/Z_{t_R}^{1/2}$, and the proper vertex renormalization

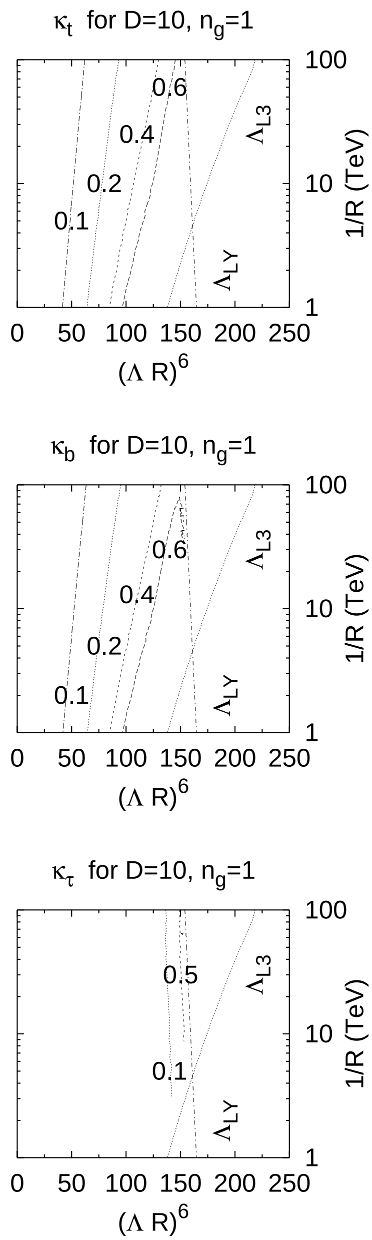

FIG. 5: The same graphs as Fig. 3 in the case of $D = 10, n_g = 1$.

constants Z_y and Z_λ. Here, we note that KK modes of the top-quark contribute the VEV of the zero mode of H (the SM Higgs boson) as well as the zero mode of the top-quark,

$$\langle H^{(0)} \rangle \propto \sum_{n=0}^{\frac{n^2}{R^2}<\Lambda^2} \langle \bar{q}_L^{(n)} t_R^{(n)} \rangle, \tag{41}$$

where $X^{(0)}$ and $X^{(n)} (n \neq 0)$ denote the zero mode and KK modes of the field X, respectively. The VEV of each condensate is thus suppressed and the mass of the top-quark thereby goes down. For more detailed analysis for predictions of m_t and m_H, we use RGEs for y and λ with the compositeness conditions [3],

$$y(\Lambda) \to \infty, \quad \frac{\lambda(\Lambda)}{y(\Lambda)^4} \to 0. \tag{42}$$

Before the full calculation of 1-loop RGEs, we analyze the property of the RGE for the top-Yukawa coupling. In the bubble approximation, we easily find the wave function renormalization constant Z_H,

$$Z_H(\mu) = \frac{y_0^2}{(4\pi)^2} N_{\rm KK}(\mu) \cdot 2^{\delta/2} \cdot N_c \ln \Lambda^2/\mu^2. \tag{43}$$

The new factors, $N_{\rm KK}$ and $2^{\delta/2}$, arise from the number of KK modes and components of the bulk fermion, respectively. On the other hand, δ pieces of gauge scalars contribute the vertex correction of the top-Yukawa coupling. Thus, the effect of Z_H becomes dominant in Eq. (40) as the number of dimensions increases. The enhancement of Z_H, of course, suppresses the top-Yukawa coupling. In order to demonstrate the suppression for the top-Yukawa coupling y, we consider the 1-loop RGE for y at the leading order of N_c:

$$(4\pi)^2 \mu \frac{dy}{d\mu} = N_{\rm KK}(\mu)\, y \left[2^{\delta/2} N_c\, y^2 - C_F (6+\delta) g_3^2 \right]. \tag{44}$$

Noting $N_{\rm KK}(\mu) \propto (\mu R)^\delta$, we obtain approximately

$$\frac{dY}{dN_{\rm KK}(\mu)} = -\frac{1}{8\pi^2 \delta} \left[2^{\delta/2} N_c - C_F (6+\delta) g_3^2 Y \right], \tag{45}$$

where we defined $Y \equiv 1/y^2$. Since the derivative of g_3^2 with respect to $N_{\rm KK}(\mu)$ is approximately given by

$$\frac{dg_3^2}{dN_{\rm KK}(\mu)} = \frac{b_3'}{8\pi^2 \delta} g_3^4, \tag{46}$$

the running effect of the gauge coupling g_3^2 is almost negligible around the compactification scale $1/R$. The top-Yukawa coupling in $\mu \sim 1/R$ is thus attracted toward the quasi IR-fixed point y_* [15, 16],

$$y_* = \sqrt{\frac{C_F (6+\delta)}{2^{\delta/2} N_c}}\, g_3, \tag{47}$$

whose value obviously decreases as δ increases. We also show the behavior of y for various boundary conditions in Fig. 6, where we used the full 1-loop RGE instead of Eq. (44). We can confirm that the top-Yukawa coupling around $1/R$ is controlled by the quasi IR-FP y_*(~ 1 for $D = 8, 10$). As a result, the problem of the prediction for m_t, $m_t > 200$ GeV, in 4-dimensions can be resolved in the TMSM with extra dimensions.

Now, we predict m_t and m_H. Within the truncated KK effective theory, we easily find RGEs for the top-Yukawa coupling y [4],

$$(4\pi)^2 \mu \frac{dy}{d\mu} = \beta_y^{\rm SM} + \beta_y^{\rm KK}, \tag{48}$$

$$\begin{aligned} \beta_y^{\rm SM} &= y \left[\left(N_c + \frac{3}{2} \right) y^2 \right. \\ &\qquad \left. -6 C_F g_3^2 - \frac{9}{4} g_2^2 - \frac{17}{12} g_Y^2 \right], \end{aligned} \tag{49}$$

$$\begin{aligned} \beta_y^{\rm KK} &= N_{\rm KK}(\mu)\, y \left[\left(2^{\delta/2} \cdot N_c + \frac{3}{2} \right) y^2 \right. \\ &\qquad -(6+\delta) C_F g_3^2 - \frac{3}{4}(3-\delta/2) g_2^2 \\ &\qquad \left. -\frac{(102-\delta)}{72} g_Y^2 \right], \end{aligned} \tag{50}$$

and for the quartic coupling λ of the Higgs boson,

$$(4\pi)^2 \mu \frac{d\lambda}{d\mu} = \beta_\lambda^{\rm SM} + \beta_\lambda^{\rm KK}, \tag{51}$$

$$\begin{aligned} \beta_\lambda^{\rm SM} &= 4 N_c \left(\lambda y^2 - y^4 \right) + 12 \lambda^2 \\ &\quad + \frac{3}{4}(3 g_2^4 + 2 g_2^2 g_Y^2 + g_Y^4) \\ &\quad -3(3 g_2^2 + g_Y^2)\lambda \end{aligned} \tag{52}$$

$$\begin{aligned} \beta_\lambda^{\rm KK} &= N_{\rm KK}(\mu) \left[2^{2+\delta/2} \cdot N_c \left(\lambda y^2 - y^4 \right) + 12 \lambda^2 \right. \\ &\quad + \frac{3+\delta}{4}(3 g_2^4 + 2 g_2^2 g_Y^2 + g_Y^4) \\ &\quad \left. -3(3 g_2^2 + g_Y^2)\lambda \right], \end{aligned} \tag{53}$$

where $\beta_{y,\lambda}^{\rm SM}$ and $\beta_{y,\lambda}^{\rm KK}$ correspond to the contributions of the zero mode and KK modes, respectively. We show solutions of the RGE for the top-Yukawa coupling in Fig. 7. Since the top-condensation is not favored in $D = 6, n_g = 1$,

[4] There are some errors in the expression of the RGE for y in Ref. [6], although they are not so significant numerically.

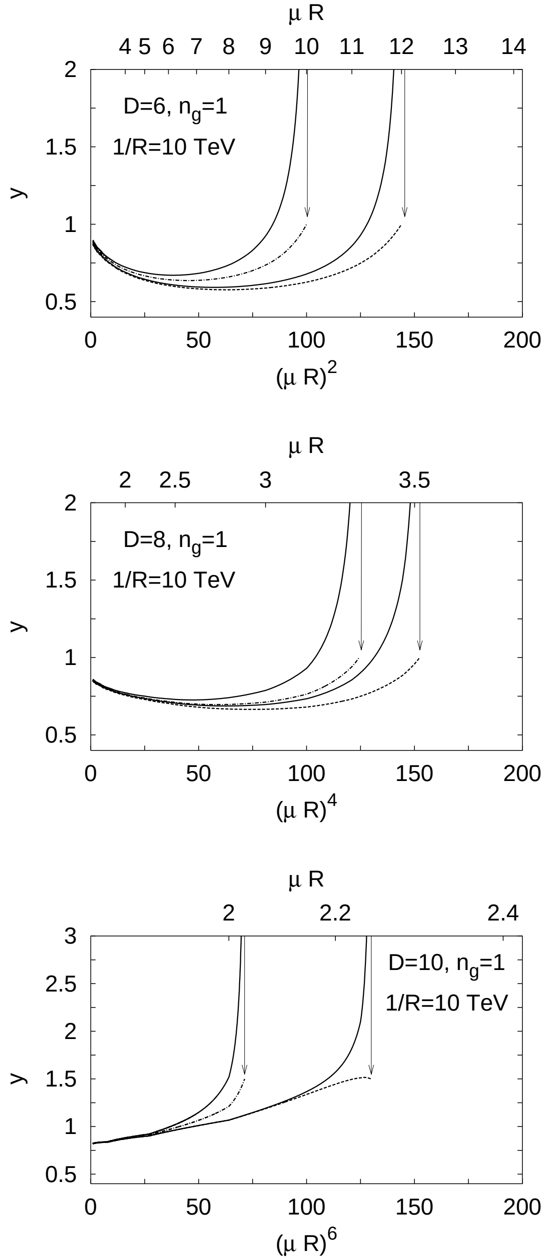

FIG. 6: The quasi IR-fixed point for the top-Yukawa coupling. The graphs from top to bottom represent the RGE flows of the top-Yukawa coupling y for $D = 6, 8, 10, n_g = 1, R^{-1} = 10$ TeV, respectively, where we used the full 1-loop RGE of y with the boundary conditions, $y(\Lambda) \to \infty$ (solid lines) and $y(\Lambda) = 1, 1, 1.5$ for $D = 6, 8, 10$ (dashed lines). We took two typical cutoffs Λ.

the solutions for $D = 8, 10, n_g = 1$ are meaningful in our scenario. Thanks to the quasi-IR-fixed point y_*, our predictions for m_t are stable. We also find that predictions for m_t are insensitive by varying the compactification scale. (See Fig. 8.) We finally obtain

$$m_t = 172 - 177 \text{ GeV}, \tag{54}$$

for $D = 8, n_g = 1$, and

$$m_t = 166 - 172 \text{ GeV}, \tag{55}$$

for $D = 10, n_g = 1$, respectively, where we took $1/R = 1 - 100$ TeV and the error range of the QCD coupling at M_Z, $\alpha_3(M_Z) = 0.1172 \pm 0.0020$. Our predictions good agree with the experimental value, 174.3 ± 5.1 GeV [14]. We also predict the mass of the Higgs boson by using RGEs of Eqs. (48) and (51) with the compositeness conditions, and find

$$m_H = 179 - 202 \text{ GeV}, \tag{56}$$

for $D = 8, n_g = 1, R^{-1} = 1 - 100$ TeV, and

$$m_H = 181 - 216 \text{ GeV}, \tag{57}$$

for $D = 10, n_g = 1, R^{-1} = 1 - 100$ TeV. (See also in Fig. 9.)

We comment that we predict $m_t \gtrsim 200$ GeV in other cases of $D = 6, 8, 10, n_g = 2, 3$. The bulk QCD coupling tends to be larger in cases of $D = 6, 8, 10, n_g = 2, 3$. This is the reason why the predictions of m_t are enhanced. We also note that the values of m_t for $D = 6, 8$ in Ref. [6] is smaller than our estimations by about $10 - 20$ GeV. The analysis for m_H is similar, too.

V. SUMMARY AND DISCUSSIONS

We have studied the DχSB in the bulk caused by bulk gauge interactions and the TMSM with extra dimensions as the phenomenological application of the bulk gauge dynamics. For this purpose, we have calculated the binding strengths of the top-, bottom-, and tau-condensates by using RGEs for gauge couplings. We showed that the analysis of the MAC in the earlier attempt [6], where all bulk gauge couplings are assumed to be equal, is not suitable and that the top-condensation takes place near the Landau pole of the bulk hypercharge. It is thus quite nontrivial whether the top-condensation is favored or not. Combining our MAC analysis with the critical binding strength κ_D^{crit} previously obtained in our papers [10, 11], we showed that the top-condensation can be favored in models with $D = 8, 10, n_g = 1$, while the tau-condensate is the MAC in $D = 6, n_g = 1$. We note that the bottom-condensation is naturally suppressed in $D = 8, n_g = 1$, whereas a fine tuning is needed to suppress the bottom-condensation in $D = 10, n_g = 1$. We emphasis that we can determine the parameter of our model, ΛR, as the energy scale realizing $\langle \bar{t}t \rangle \neq 0$, in sharp contrast to earlier approaches of Ref. [6, 13] where the cutoff is treated as a free parameter. By using the RGE for the top-Yukawa coupling and the compositeness conditions at the cutoff satisfying $\kappa_t(\Lambda) \simeq \kappa_D^{\text{crit}}$, we have predicted the top-quark mass m_t:

$$m_t = 172 - 177 \text{ GeV} \tag{58}$$

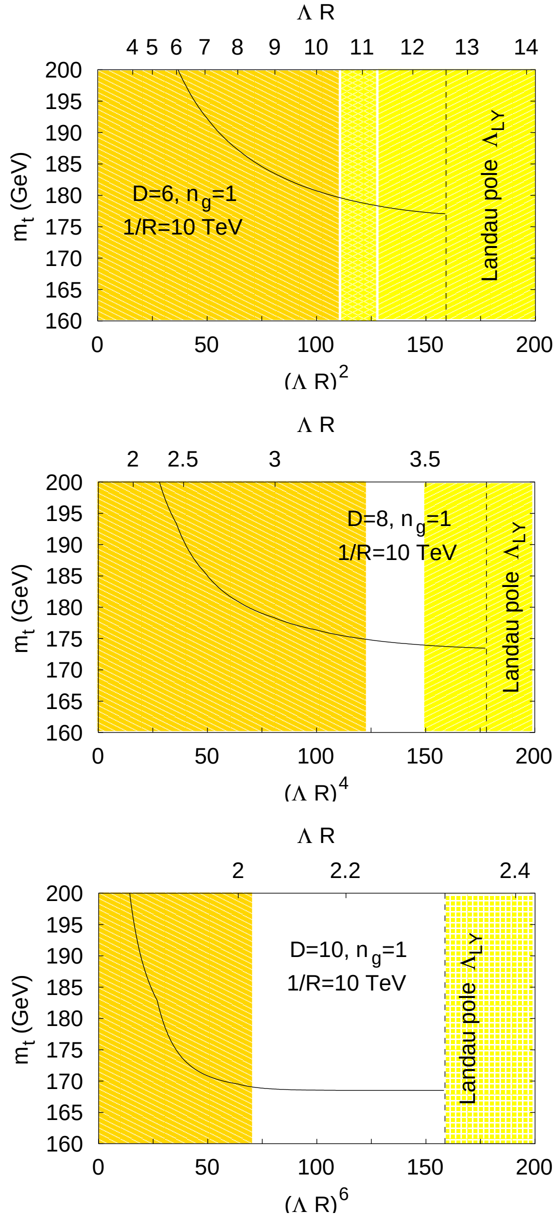

FIG. 7: Solutions of the RGE for the top-Yukawa coupling. The graphs from top to bottom show the top-quark mass ($m_t = v \cdot y(m_t)/\sqrt{2}$) for $D = 6, n_g = 1, R^{-1} = 10$ TeV, $D = 8, n_g = 1, R^{-1} = 10$ TeV, and $D = 10, n_g = 1, R^{-1} = 10$ TeV. In all graphs, the unshaded regions are preferable for the top-condensation. We used $\alpha_3(M_Z) = 0.1172$, $\alpha_2(M_Z) = 0.033813$, and $\alpha_Y(M_Z) = 0.010166$.

for $D = 8, n_g = 1$, and

$$m_t = 166 - 172 \text{ GeV} \tag{59}$$

for $D = 10, n_g = 1$, respectively, where we took $1/R = 1 - 100$ TeV and the error range of the QCD coupling as $\alpha_3(M_Z) = 0.1172 \pm 0.0020$.

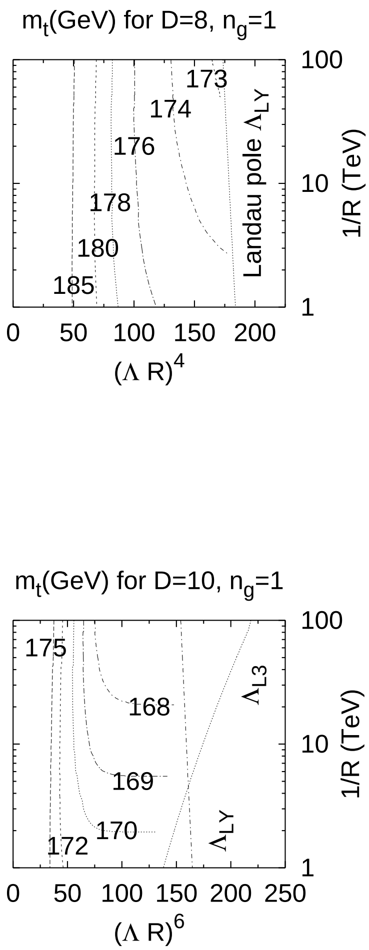

FIG. 8: Predictions of the top-quark mass $m_t(= v \cdot y(m_t)/\sqrt{2})$ for $D = 8, 10, n_g = 1$. The horizontal and vertical lines represent $(\Lambda R)^\delta$ and the compactification radius R^{-1}, respectively. We used $\alpha_3(M_Z) = 0.1172$, $\alpha_2(M_Z) = 0.033813$, and $\alpha_Y(M_Z) = 0.010166$. We do not show the graph for $D = 6, n_g = 1$, because the top-condensation is not favored in our scenario.

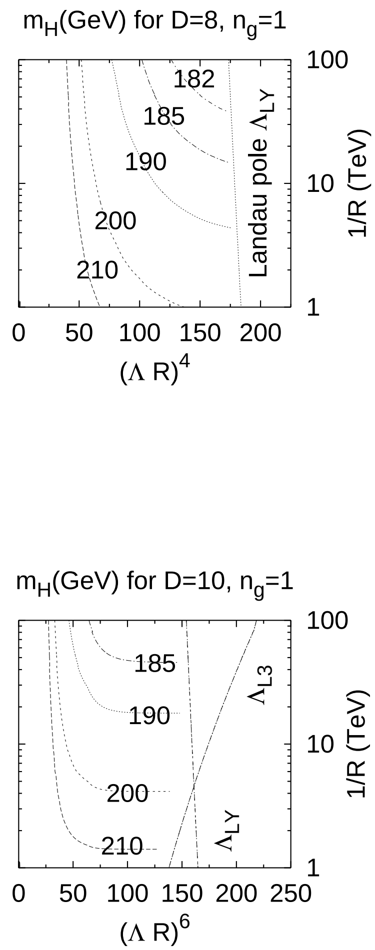

FIG. 9: Predictions of the Higgs boson mass $m_H(= v \cdot \sqrt{\lambda(m_H)})$ for $D = 8, 10, n_g = 1$. The horizontal and vertical lines represent $(\Lambda R)^\delta$ and the compactification radius R^{-1}, respectively. We used $\alpha_3(M_Z) = 0.1172$, $\alpha_2(M_Z) = 0.033813$, and $\alpha_Y(M_Z) = 0.010166$. We do not show the graph for $D = 6, n_g = 1$, because the top-condensation is not favored in our scenario.

Our predictions for m_t are stable thanks to the quasi IR-FP y_* and consistent with the experimental value of m_t, $m_t = 174.3 \pm 5.1$ GeV. Since the value of y_* is approximately given by $y_* = g_3 \cdot \sqrt{C_F(6+\delta)/(2^{\delta/2}N_c)}$, the mass of the top-quark tends to decrease as the number of dimensions increases. This is one of reason why the problem of the prediction for m_t larger than 200 GeV in 4-dimensions is resolved in extra dimensions. Since the suppression factor $2^{\delta/2}$ in y_* comes from the number of components of the chiral fermion in the D-dimensional bulk, it is essential that the top-condensation takes place in the bulk. Although the solution of RGE in $D = 6, n_g = 1$, $m_t = 176 - 182$ GeV,is also consistent with the experimental value, we need to introduce the attractive 4-top interaction in the bulk in order to enhance the binding strength of the top-condensate. In addition, we found again $m_t \gtrsim 200$ GeV for $D = 6, 8, 10, n_g = 2, 3$. Since the bulk QCD coupling grows as the number of bulk fermions increases, the top mass also tends to be larger than the values for $n_g = 1$. As for the Higgs boson mass, we predicted

$$m_H = 179 - 202 \text{ GeV} \tag{60}$$

for $D = 8, n_g = 1$, and

$$m_H = 181 - 216 \text{ GeV} \tag{61}$$

for $D = 10, n_g = 1$, respectively. The Higgs boson with the mass, $m_H \sim 180 - 220$ GeV, can be easily observed at collider experiments such as the LHC.

Some issues remain unsolved. In particular, the explicit breaking of the D-dimensional Lorentz symmetry, whose effects are not taken into account in the estimation of $\kappa_D^{\rm crit}$, may be important, because the cutoff Λ is not so large compared with the compactification scale $1/R$. Since our scenario is strongly depend on the value of $\kappa_D^{\rm crit}$, it is important to determine precisely $\kappa_D^{\rm crit}$. A regular strategy is that we investigate the effective theory on the 3-brane including effects of KK modes. It is, however, quite difficult to perform such an analysis, because the gap equation is not a closed form including only zero mode of fermions. In this paper, we have taken $\kappa_D^{\rm crit}$ most conservatively as minimal values among available ones. If more reliable values of $\kappa_D^{\rm crit}$ are significantly larger, our scenario, i.e., the DχSB thanks to the bulk gauge dynamics, may be broken down. In such a case, we may introduce 4-fermion interactions, for example, so as to get out of the problem. Then, we need to study the phase structure of the gauged Nambu-Jona-Lasinio model. The investigation will be performed elsewhere. [25]

APPENDIX A: ORBIFOLD COMPACTIFICATION AND NUMERICAL ANALYSIS FOR $N_{\rm KK}$

We have investigated the top-condensation in the bulk. Since a chiral fermion in the bulk ($D > 4$) has four or more components, we compactify extra dimensions on an orbifold so that unwanted components are projected out by its boundary conditions. Of course, gauge bosons also have unwanted components, i.e., gauge scalars. For gauge bosons A_M, we impose the following Z_2 symmetry as usual,

$$A_\mu(x^\mu, -y^j) = +A_\mu(x^\mu, y^j) \tag{A1}$$

for conventional pieces, and

$$A_j(x^\mu, -y^j) = -A_j(x^\mu, y^j) \tag{A2}$$

for gauge scalars, where we decomposed the space-time coordinate into conventional dimensions and extra ones:

$$\begin{aligned} x^M &= (x^\mu, y^j), \quad M = 0,1,2,3,5,6,\cdots,D, \\ \mu &= 0,1,2,3, \quad j = 5,6,\cdots,D. \end{aligned} \tag{A3}$$

For chiral fermions in the bulk, such a discrete symmetry may be nontrivial. We thus describe concretely a systematic procedure to find a desirable orbifold compactification.

Let us consider the minimal case $D = 6$ for simplicity. The chiral projection operators in six dimensions are given by

$$\frac{1 \pm \Gamma_\chi}{2}, \qquad \Gamma_\chi \equiv \Gamma^0\Gamma^1\Gamma^2\Gamma^3\Gamma^5\Gamma^6, \tag{A4}$$

and the chiral fermions $\psi_\pm$ satisfy the relation

$$\Gamma_\chi \psi_\pm = \pm\psi_\pm. \tag{A5}$$

We compactify extra dimensions to a torus with a universal compactification radius R:

$$\begin{aligned} \psi_\pm(x^\mu, y^5, y^6) &= \psi_\pm(x^\mu, y^5 + 2\pi R, y^6) \\ &= \psi_\pm(x^\mu, y^5, y^6 + 2\pi R). \end{aligned} \tag{A6}$$

The chiral fermion in $D = 6$ is then decomposed into KK modes:

$$\begin{aligned} &\psi_\pm(x^\mu, y^j) = \\ &\quad \sum_{n_5,n_6} \psi_\pm^{(n_5,n_6)}(x^\mu) \exp\left[i\frac{n_5 y^5 + n_6 y^6}{R}\right]. \end{aligned} \tag{A7}$$

We next introduce the four-dimensional chirality matrix γ_5,

$$\gamma_5 \equiv i\Gamma^0\Gamma^1\Gamma^2\Gamma^3, \tag{A8}$$

which satisfies

$$\gamma_5\gamma_5 = 1 \tag{A9}$$

and

$$\gamma_5\Gamma_\chi = \Gamma_\chi\gamma_5 = -i\Gamma^5\Gamma^6. \tag{A10}$$

The chiral fermion in 4-dimensions is defined by the chiral projection of γ_5,

$$(\psi)_{R,L} \equiv \frac{1 \pm \gamma_5}{2}\psi. \tag{A11}$$

Now, we impose the boundary condition

$$\psi_\pm(x, -y^5, -y^6) = -i\Gamma^5\Gamma^6\psi_\pm(x, y^5, y^6). \tag{A12}$$

By definition of $\psi_\pm$ and using Eq. (A10), we find that the Z_2 projection of Eq. (A12) is equivalent to

$$\psi_\pm(x, -y^5, -y^6) = \pm\gamma_5\psi_\pm(x, y^5, y^6). \quad \text{(A13)}$$

Under this Z_2 symmetry, 4-dimensional chiral fermions behave as

$$(\psi_+)_R \to +(\psi_+)_R, \quad (\psi_+)_L \to -(\psi_+)_L, \text{(A14)}$$

and

$$(\psi_-)_R \to -(\psi_-)_R, \quad (\psi_-)_L \to +(\psi_-)_L. \text{(A15)}$$

We thus identify right(left)-handed particles in the SM as $\psi_+(\psi_-)$. In the same way, we can reduce chiral fermions in $D = 2k + 2$ dimensions to those in $D = 2k$ dimensions. For more general procedures, see, e.g., Ref. [10].

Let us count the total number of KK modes below μ in our orbifold compactification. For simplicity, we study a bulk scalar field ϕ having the zero mode, $\phi(x^\mu, -y^j) = +\phi(x^\mu, y^j)$. The effective Lagrangian $\mathcal{L}_{D-2}$ in $(D-2)$-dimensions is derived from the D-dimensional one $\mathcal{L}_D$:

$$\mathcal{L}_{D-2} = \frac{1}{2}\int_{-\pi R}^{\pi R} dy^{D-1} \int_{-\pi R}^{\pi R} dy^D \mathcal{L}_D, \quad \text{(A16)}$$

where the factor 1/2 arises from the Z_2-symmetry. Our scalar field $\phi(x^M)$ is then decomposed into its KK modes as follows:

$$\begin{aligned}\phi(x^\mu, y^i, y^{D-1}, y^D) \;&=\; \phi^{(0,0)} \\ &+ \sum_{n_{D-1}>0} \phi^{(n_{D-1},0)} c_{D-1} + \sum_{n_D>0} \phi^{(0,n_D)} c_D \\ &+ \sum_{n_{D-1},n_D>0} \phi^{(n_{D-1},n_D)} c_{D-1}c_D \\ &+ \sum_{n_{D-1},n_D>0} \phi^{(n_{D-1},n_D)} s_{D-1}s_D \quad \text{(A17)}\end{aligned}$$

where we omitted the trivial argument (x^μ, y^i), $i = 5, 6, \cdots, D-2$ in $(D-2)$-dimensional KK modes such as $\phi^{(n_{D-1},n_D)}$ and we defined

$$c_i \equiv \cos\left[\frac{n_i y^i}{R}\right], s_i \equiv \sin\left[\frac{n_i y^i}{R}\right]. \quad \text{(A18)}$$

We note that Z_2-odd parts in $\phi(x^M)$ such as $\phi^{(n_{D-1},n_D)} s_{D-1}c_D$ are projected out by our orbifold compactification. After the dimensional reduction Eq. (A16), KK modes $\phi^{(n,0)}$ and $\phi^{(0,n)}$ have a same mass spectrum $M_{\rm KK}$ characterized by one positive integer n, $M_{\rm KK} = n^2/R^2$. Similarly, the fourth and fifth terms in Eq. (A17) acquire same KK masses characterized by two positive integers n_{D-1} and n_D, $M_{\rm KK} = (n_{D-1}^2 + n_D^2)/R^2$. So as to avoid complexity, we introduce a notation for $(D-2)$-dimensional KK modes characterized by some integers,

$$\phi_{D,2}^{[k_1,k_2,\cdots]}, \quad \text{(A19)}$$

i.e., $\phi^{(n,0)}, \phi^{(0,n)} \in \phi_{D,2}^{[k_1]}$ and so on. The zero mode in $(D-2)$-dimensions is represented as $\phi_{D,2}^0$. An important point is that one zero mode $\phi_{D,2}^0$ and two pieces of $\phi_{D,2}^{[k_1]}$ and $\phi_{D,2}^{[k_1,k_2]}$ are left in the decomposition Eq. (A17):

$$\#\phi_{D,2}^0 = 1,\ \#\phi_{D,2}^{[k_1]} = 2,\ \#\phi_{D,2}^{[k_1,k_2]} = 2. \quad \text{(A20)}$$

While our procedure to obtain a 4-dimensional theory from a 6-dimensional one is ended here, we continue the reduction Eq. (A16) in $D = 8, 10$. After twice reduction, $(D-4)$-dimensional KK modes $\phi_{D,4}^{[k_1]}$ characterized by one positive integer come from two KK modes of $\phi_{D,2}^0$ and one zero mode of two pieces of $\phi_{D,2}^{[k_1]}$, i.e., $\#\phi_{D,4}^{[k_1]} = 4$. The number of $\phi_{D,4}^{[k_1,k_2]}$ is more complicated: The zero mode of $\phi_{D,2}^{[k_1,k_2]}$ also contributes it as well as KK modes of $\phi_{D,2}^0$ and $\phi_{D,2}^{[k_1]}$. In this way, we find

$$\#\phi_{D,4}^0 = 1,\ \#\phi_{D,4}^{[k_1]} = 4,\ \#\phi_{D,4}^{[k_1,k_2]} = 8,$$

$$\#\phi_{D,4}^{[k_1,k_2,k_3]} = 8,\ \#\phi_{D,4}^{[k_1,k_2,k_3,k_4]} = 4. \quad \text{(A21)}$$

After triple reduction, we obtain similarly

$$\#\phi_{D,6}^0 = 1,\ \#\phi_{D,6}^{[k_1]} = 6,\ \#\phi_{D,6}^{[k_1,k_2]} = 18,$$

$$\#\phi_{D,6}^{[k_1,k_2,k_3]} = 32,\ \#\phi_{D,6}^{[k_1,k_2,k_3,k_4]} = 36,$$

$$\#\phi_{D,6}^{[k_1,k_2,k_3,k_4,k_5]} = 24,\ \#\phi_{D,6}^{[k_1,k_2,k_3,k_4,k_5,k_6]} = 8. \quad \text{(A22)}$$

The total number of KK modes below the renormalization point μ in the 4-dimensional effective theory is then given by

$$\begin{aligned}N_{\rm KK}(\mu) = \\ &\sum_{k_1>0}^{k_1^2/R^2<\mu^2} \#\phi_{D,D-4}^{[k_1]} + \sum_{k_1,k_2>0}^{(k_1^2+k_2^2)/R^2<\mu^2} \#\phi_{D,D-4}^{[k_1,k_2]} \\ &+ \sum_{k_1,k_2,k_3>0}^{(k_1^2+k_2^2+k_3^2)/R^2<\mu^2} \#\phi_{D,D-4}^{[k_1,k_2,k_3]} + \cdots . \quad \text{(A23)}\end{aligned}$$

We use the counting rules Eqs. (A20), (A21), and (A22) for $D = 6, 8$ and $D = 10$, respectively.

We count numerically the total number of KK modes below μ and show the result in Fig. 10. In our analysis, the DχSB takes place around $N_{\rm KK}(\Lambda) \sim 100$ for $D = 6, 8, 10, n_g = 1$. However, the cutoffs Λ corresponding to $N_{\rm KK}(\Lambda) \sim 100$ are depend on the number of extra dimensions, $\Lambda R \sim 10, 3, 2$ for $D = 6, 8, 10$. We note that the analytical expression for $N_{\rm KK}$ in Eq. (6) does not work well around $\Lambda R \sim 2 - 3$. (See also Fig. 10.) It causes discrepancy of RGE flows of gauge couplings between the numerical solution and the analytical one for $D = 8, 10$. (See also Fig. 1.)

[1] V. A. Miransky, M. Tanabashi, and K. Yamawaki, Phys. Lett. **B 221**, 177 (1989); Mod. Phys. Lett. **A 4**, 1043 (1989).

[2] Y. Nambu, Enrico Fermi Institute Report No. 89-08, 1989; in *Proceedings of the 1989 Workshop on Dynamical Symmetry Breaking*, edited by T. Muta and K. Yamawaki (Nagoya University, Nagoya, Japan, 1990).

[3] W. A. Bardeen, C. T. Hill and M. Lindner, Phys. Rev. **D41**, 1647 (1990).

[4] M. Hashimoto, Prog. Theor. Phys. **100**, 781 (1998).

[5] C. T. Hill, and E. H. Simmons, hep-ph/0203079.

[6] N. Arkani-Hamed, H. C. Cheng, B. A. Dobrescu and L. J. Hall, Phys. Rev. **D62**, 096006 (2000), [arXiv:hep-ph/0006238].

[7] N. Arkani-Hamed, S. Dimopoulos and G. Dvali, Phys. Lett. **B429** (1998) 263; Phys. Rev. **D59** (1999) 086004; I. Antoniadis, N. Arkani-Hamed, S. Dimopoulos and G. Dvali, Phys. Lett. **B436** (1998) 257.

[8] K. R. Dienes, E. Dudas and T. Gherghetta, Phys. Lett. **B436**, 55 (1998), [arXiv:hep-ph/9803466].

[9] K. R. Dienes, E. Dudas and T. Gherghetta, Nucl. Phys. **B537**, 47 (1999), [arXiv:hep-ph/9806292].

[10] M. Hashimoto, M. Tanabashi and K. Yamawaki, Phys. Rev. **D64**, 056003 (2001), [arXiv:hep-ph/0010260].

[11] V. Gusynin, M. Hashimoto, M. Tanabashi and K. Yamawaki, Phys. Rev. **D65**, 116008 (2002), [arXiv:hep-ph/0201106].

[12] S. Raby, S. Dimopoulos and L. Susskind, Nucl. Phys. **B169**, 373 (1980).

[13] A. B. Kobakhidze, Phys. Atom. Nucl. **64**, 941 (2001), [Yad. Fiz. **64**, 1010 (2001)], [arXiv:hep-ph/9904203].

[14] K. Hagiwara *et al.* [Particle Data Group Collaboration], Phys. Rev. **D66**, 010001 (2002).

[15] C. T. Hill, Phys. Rev. **D24**, 691 (1981).

[16] C. T. Hill, C. N. Leung, and S. Rao, Nucl. Phys. **B262**, 517 (1985).

[17] A. Manohar and H. Georgi, Nucl. Phys. **B234**, 189 (1984).

[18] Z. Chacko, M. A. Luty and E. Pontón, JHEP **0007**, 036 (2000), [arXiv:hep-ph/9909248].

[19] H. Pagels and S. Stokar, Phys. Rev. **D20**, 2947 (1979).

[20] V. A. Miransky, Sov. J. Nucl. Phys. **38**, 280 (1983), [Yad. Fiz. **38**, 468 (1983)].

[21] K. Higashijima, Phys. Rev. **D29**, 1228 (1984).

[22] T. Kugo and M. G. Mitchard, Phys. Lett. **B282**, 162 (1992).

[23] W. A. Bardeen, C. N. Leung and S. T. Love, Phys. Rev. Lett. **56**, 1230 (1986).

[24] C. N. Leung, S. T. Love and W. A. Bardeen, Nucl. Phys. B **273**, 649 (1986).

[25] V. P. Gusynin, M. Hashimoto, M. Tanabashi and K. Yamawaki, in preparation.

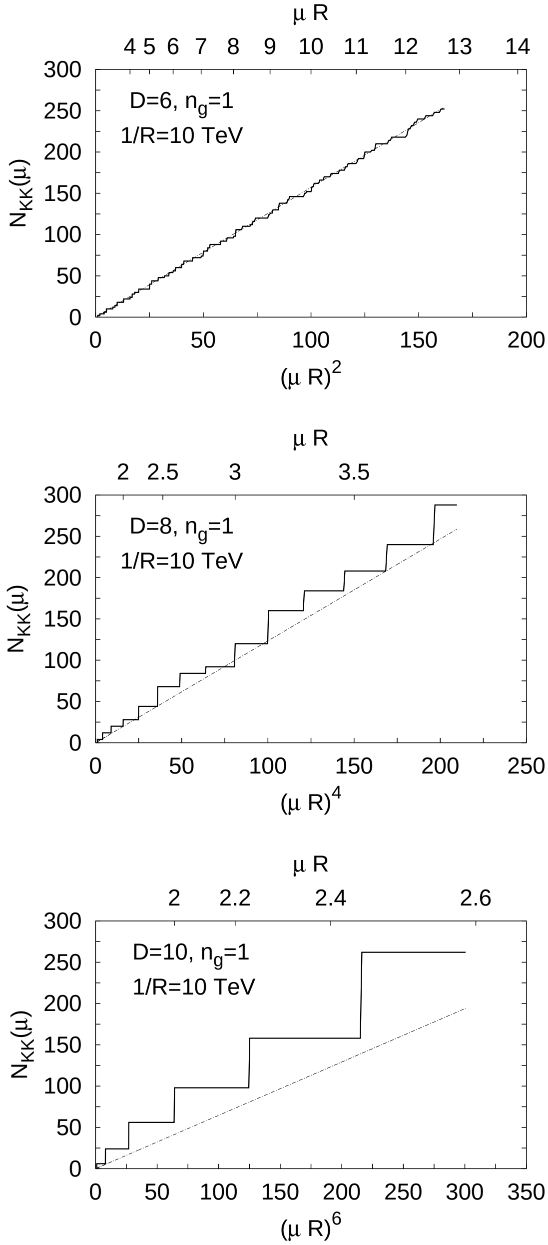

FIG. 10: Total number of KK modes $N_{\rm KK}(\mu)$ below the renormalization point μ. The graphs from top to bottom show $N_{\rm KK}(\mu)$ for $D = 6, 8, 10, n_g = 1$. In all graphs, bold and dotted lines represent the numerical analysis of $N_{\rm KK}(\mu)$ and the approximate expression Eq. (6) for $\mu R \gg 1$, respectively.